Neuromol Med (2013) 15:504–514
DOI 10.1007/s12017-013-8236-z

ORIGINAL PAPER

Mechanism of Action for NNZ-2566 Anti-inflammatory Effects Following PBBI Involves Upregulation of Immunomodulator ATF3

Casandra M. Cartagena · Katie L. Phillips · Garry L. Williams · Melissa Konopko · Frank C. Tortella · Jitendra R. Dave · Kara E. Schmid

Received: 1 March 2013 / Accepted: 24 May 2013 / Published online: 14 June 2013

Abstract The tripeptide glycine–proline–glutamate analogue NNZ-2566 (Neuren Pharmaceuticals) demonstrates neuroprotective efficacy in models of traumatic brain injury. In penetrating ballistic-like brain injury (PBBI), it significantly decreases injury-induced upregulation of inflammatory cytokines including TNF-α, IFN-γ, and IL-6. However, the mechanism by which NNZ-2566 acts has yet to be determined. The activating transcription factor-3 (ATF3) is known to repress expression of these inflammatory cytokines and was increased at the mRNA and protein level 24-h post-PBBI. This study investigated whether 12 h of NNZ-2566 treatment following PBBI alters *atf3* expression. PBBI alone significantly increased *atf3* mRNA levels by 13-fold at 12 h and these levels were increased by an additional fourfold with NNZ-2566 treatment. To confirm that changes in mRNA translated to changes in protein expression, ATF3 expression levels were determined in vivo in microglia/macrophages, T cells, natural killer cells (NKCs), astrocytes, and neurons. PBBI alone significantly increased ATF3 in microglia/macrophages (820 %), NKCs (58 %), and astrocytes (51 %), but decreased levels in T cells (48 %). NNZ-2566 treatment further increased ATF3 protein expression in microglia/macrophages (102 %), NKCs (308 %), and astrocytes (13 %), while reversing ATF3 decreases in T cells. Finally, PBBI increased ATF3 levels by 55 % in neurons and NNZ-2566 treatment further increased these levels an additional 33 %. Since increased ATF3 may be an innate protective mechanism to limit inflammation following injury, these results demonstrating that the anti-inflammatory and neuroprotective drug NNZ-2566 increase both mRNA and protein levels of ATF3 in multiple cell types provide a cellular mechanism for NNZ-2566 modulation of neuroinflammation following PBBI.

Keywords NNZ-2566 · Penetrating ballistic-like brain injury · Traumatic brain injury

Electronic supplementary material The online version of this article (doi:10.1007/s12017-013-8236-z) contains supplementary material, which is available to authorized users.

C. M. Cartagena (✉) · K. L. Phillips · G. L. Williams · M. Konopko · F. C. Tortella · J. R. Dave · K. E. Schmid
Brain Trauma Neuroprotection and Neurorestoration Branch, Center for Military Psychiatry and Neuroscience, Walter Reed Army Institute of Research, 503 Robert Grant Avenue, Silver Spring, MD 20910, USA
e-mail: casandra.cartagena@us.army.mil

K. L. Phillips
e-mail: katie.phillips1@us.army.mil

G. L. Williams
e-mail: garryleejr@hotmail.com

M. Konopko
e-mail: melissa.konopko@gmail.com

F. C. Tortella
e-mail: frank.c.tortella@us.army.mil

J. R. Dave
e-mail: jitendra.ramanlal.dave@us.army.mil

K. E. Schmid
e-mail: kara.schmid@us.army.mil

Introduction

NNZ-2566 is an analogue of the endogenous tripeptide glycine–proline–glutamate (GPE) with improved biostability (Bickerdike et al. 2009). It has been shown to be neuroprotective following penetrating ballistic-like brain injury (PBBI) by improving motor function (Lu et al. 2009a) and reducing the incidence, frequency, and total duration of PBBI-induced non-convulsive seizures (Lu et al. 2009b).

NNZ-2566 has also been shown to be neuroprotective following acute focal stroke (Bickerdike et al. 2009) and is currently in a Phase 2 clinical trial for the treatment for moderate and severe traumatic brain injury (TBI). Although it has been suggested that the parent molecule GPE is an antagonist to the *N*-methyl-D-aspartic acid receptor (NMDA-R), neither NNZ-2566 nor GPE bind primarily to NMDA-R (Bickerdike et al. 2009; Saura et al. 1999) and NNZ-2566 does not protect against glutamate excitotoxicity in vitro (Lu et al. 2009b). A primary mechanistic target for NNZ-2566 has yet to be determined, although a wide assortment of receptors and enzymes have been ruled out (Bickerdike et al. 2009). However, there is good evidence that NNZ-2566 has anti-inflammatory properties as demonstrated by reduced microglial activation and decreased neutrophil infiltration after PBBI (Lu et al. 2009a). In addition, NNZ-2566 treatment after PBBI inhibited the injury-induced upregulation in pro-inflammatory cytokines interleukin-1beta (IL-1β), interleukin-6 (IL-6), tumor necrosis factor alpha (TNF-α), and interferon gamma (IFN-γ) (Wei et al. 2009). This suggests that NNZ-2566 may impart neuroprotection by modulating the immune response following TBI.

One possible mechanism through which NNZ-2566 could produce this immunomodulation is through the regulation of the activating transcription factor-3 (ATF3). ATF3 is a member of the ATF/CREB family and functions as a transcription repressor (Chen et al. 1994). Studies in macrophages indicate that ATF3 reduces pro-inflammatory cytokine production by attenuating the toll-like receptor (TLR)-induced transcription of CCAAT/enhancer-binding protein delta (Litvak et al. 2009). Further, macrophages isolated from $ATF3^{-/-}$ knockout mice have elevated levels of TNF-α, IL-6, and IL-12 following TLR activation in comparison with wild-type controls, indicating that ATF3 negatively regulates the expression of these pro-inflammatory cytokines. In addition, similar studies of stimulated natural killer cells (NKCs) from $ATF3^{-/-}$ mice demonstrated increased IFN-γ production in comparison with wild-type controls, demonstrating that IFN-γ production is also negatively regulated by ATF3 (Rosenberger et al. 2008). Given these previous findings, the reduction in microglial activation and inhibition of pro-inflammatory cytokines with NNZ-2566 treatment after TBI may be due to modulation of ATF3. In this study, we investigate the effects of NNZ-2566 treatment on ATF3 expression following PBBI.

Materials and Methods

Animals

Male Sprague–Dawley rats (250–300 g) were used in these experiments. All surgical procedures were performed under anesthesia (2 % isoflurane delivered in oxygen). All procedures were approved by the Institutional Animal Care and Use Committee of WRAIR. Research was conducted in compliance with the Animal Welfare Act and other federal statutes and regulations relating to animals and experiments involving animals and adheres to principles stated in the Guide for the Care and Use of Laboratory Animals, NRC Publication, 2011 edition.

Penetrating Ballistic-Like Brain Injury

The unilateral frontal PBBI model, which mimics the ballistic dynamics of a bullet or fragment wound to the head (Williams et al. 2005, 2006b), was induced by stereotactic insertion of a custom probe through the right frontal cortex. A temporary cavity was formed by the rapid inflation/deflation (i.e., <40 ms) of an elastic balloon attached to the end of the probe. The PBBI apparatus consisted of a computer-controlled hydraulic pressure generator (Mitre Corp., McLean, VA, USA), a PBBI probe, and a stereotaxic frame equipped with a custom-designed probe holder as previously described (Lu et al. 2009a, 2011; Williams et al. 2005). The injury tract began at −3 mm bregma and continued through +3 mm bregma (Williams et al. 2005), and the injury severity was determined by the size of the balloon. The balloon diameter calibrated to 0.63 cm expansion represented 10 % of the total rat brain volume (10 % PBBI). As described previously, sham animals received only a craniotomy (Williams et al. 2005, 2006b). Separate groups of animals were used for mRNA analysis, Western blot analysis, and fluorescence immunostain analysis. At the end of each time point (4, 12, 24 h, 3 or 7 days), brains for mRNA analysis were sliced coronally and the half ipsilateral to the injury was snap-frozen and stored at −80 °C for later analysis. At the end point (24 h), brains for Western blot were sliced coronally and the half ipsilateral to the injury was snap-frozen and stored at −80 °C for later analysis. At the end time point (24 h), brains for fluorescence immunostain analysis were perfused with isotonic saline followed by 4 % paraformaldehyde, cryoprotected in sucrose, and then snap-frozen, sectioned and stored at −80 °C for later analysis.

RNA Isolation

A 3-mm (100 μg) coronal section starting at the frontal pole of the brain was obtained and the ipsilateral hemisection was used for RNA isolation from sham or PBBI animals. Purified total RNA was isolated using the RNeasy Lipid Tissue Mini Kit (74804, Qiagen) according to the manufacturer's directions. Samples were eluted in RNAs/DNAse-free water and stored at −80 °C.

PCR Targeted Transcription Factor Array

Random primers (RT2 First-strand Kit, SA Biosystems) were used to generate cDNA for array analysis per manufacture's directions. Pooled RNA samples from 5 to 6 animals per group (Sham or PBBI) using equal total RNA from each animal were used for the analysis. Resulting cDNA was applied to RT^2 Profiler PCR Array System per manufacture's specifications. Each gene was represented by one well on the array. Fold changes were determined using SA Biosystems RT2 Profiler PCR Array Data Analysis web-based software using equation $2^{-\Delta\Delta C_t}$.

Western Blot

Samples were analyzed at 24-h post-injury for both groups (sham and PBBI ($n = 8$)]. Tissue was homogenized in RIPA buffer containing HALT protease inhibitors (Thermo Scientific). Total protein was normalized based on BCA assay. Loading efficiency and transfer were confirmed by Ponceau S staining. Blots were blocked in 5 % milk, probed with anti-ATF3 (1:1,000, Santa Cruz) primary antibody and donkey anti-rabbit (1:25,000, GE healthcare) secondary antibody, and detected using ECL. Blots were reprobed with anti-beta-actin antibody to control for protein loading. Band intensity was measured using an LAS4000 docking station and ImageQuantTL software (GE Healthcare).

NNZ-2566 Treatment

For all groups (vehicle-treated sham, vehicle-treated PBBI, and NNZ-2566-treated PBBI), treatments were initiated 30-min post-injury. Six animals were used for each group at each post-injury time point. Treatment duration, end time points, and procedures were in accordance with previously published studies on NNZ-2566 treatment following PBBI to facilitate direct comparisons to earlier findings (Lu et al. 2009a, b; Wei et al. 2009). Briefly, using an indwelling intravenous (i.v.) catheter on a free-moving tether, an i.v. bolus injection of 10 mg/kg NNZ-2566 or 1 ml/kg vehicle (saline) was given followed by continuous infusion of NNZ-2566 at 3 mg/kg/h or an equal volume of vehicle either through 4-h post-injury (4-h groups) or through 12-h post-injury (12- and 24-h groups, 3- and 7-day groups). Animals were awake and alert with access to food and water during infusions. Following infusion, they were returned to their home cages until the end time point.

cDNA Synthesis for Real-Time PCR

cDNA was synthesized using 3 μg of total RNA and oligo(dt) primers according to the manufacture's directions (AffinityScript QPCR cDNA Synthesis kit, Stratagene). The reaction was incubated at 25 °C for 5 min, 42 °C for 45 min, 95 °C for 5 min, 4 °C for 5 min. cDNA was diluted 1:10 in RNAse/DNase-free water and stored at −20 °C.

Real-Time PCR

Relative amounts of mRNA were measured by real-time PCR using Taqman assay Rn00563784_m1 (Applied Biosystems) against *atf3* (NM_012912.1). Each sample was tested in triplicate. We have confirmed that there is no significant PBBI effect on β-actin mRNA threshold cycle (C_t) levels (data not shown). Therefore, ΔC_t levels for β-actin were used as an endogenous control to normalize ΔC_t levels for each sample and relative quantities were calculated using the formula $RQ = 2^{-\Delta\Delta C_t}$. Analysis of real-time amplification data was performed and relative quantities were calculated using 7500 software Version 2.0.1 (Applied Biosystems).

Fluorescence Immunostaining

All fluorescence immunostaining was done on 16 μ coronal slices adhered to superfrost plus glass slides. A comparable coronal slice from sham and PBBI tissue with hematoxylin and eosin staining (4× objective) is included in Supplemental Figure 1 to demonstrate the injury site area. More extensive descriptions of the full PBBI injury along the injury track can be found in previous publications on this model (Amiry-Moghaddam et al. 2003; Williams et al. 2005, 2006a, b, 2007). All incubations were performed using the Shannon coverslip apparatus. Tissue was washed with 1 ml PBS containing 0.01 % Triton X-100 (PBST-100) and then blocked for 2 h at room temperature in 200 μl 10 % fetal bovine serum plus 0.01 % sodium azide in PBST-100. Tissue was then incubated overnight with 200 μl rabbit anti-ATF3 (1:50, sc-188, Santa Cruz) and one cell-type-specific antibody in blocking solution at 4 °C. The cell-type-specific primary antibodies were as follows: (neurons) chicken anti-NeuN (1:200, NUN, Aves Labs), (microglia) mouse anti-OX42 (1:100, Serotec), (astrocytes) mouse anti-GFAP (1:100, MAB3402, Millipore), (T cells) mouse anti-CD3 (1:100, 550295, BD Pharmingen), (NK cells) mouse anti-NK Cell (1:100, ANK44, Abcam). Tissue was washed with 2 ml PBST-100 and incubated for 2 h in room temperature in the dark with the Dy 405 anti-chicken (1:100, Jackson ImmunoResearch) and either Rhodamine Red anti-chicken (1:100, Jackson ImmunoResearch) or Alexa 568 anti-mouse (1:100, Molecular Probes). Tissue was washed with 2 ml PBST-100 followed by 1 ml PBS and then mounted with Fluoramount G (Electron Microscopy Sciences). Signal was captured with a 20× objective on separate channels with a Zeiss LSM 700 confocal microscope.

Relative ATF3 Levels

The quantitative analysis of ATF3 expression with specific cell types in vivo was based on the previously published method (Cartagena et al. 2008). Using fluorescent co-staining for ATF3 and a cell-type-specific marker, a 1 μ slice at center of the field along the *z*-axis was obtained using Zeiss Zen 2011 software. Six fields at the injury site were obtained from each animal ($n = 6$ animals per group, for a total of 36 fields per group). Signal from Dy405 (ATF3) channel and either the Rhodamine Red (chicken antibody against NeuN) or Alexa 568 (mouse antibodies against GFAP, OX42, CD3, or NKcells) were isolated separately for each field and saved as 16-bit grayscale images. Images were then analyzed using Image J software. Using the Rhodamine Red or Alexa 568 images, location of cells of a specific cell type were located and coordinates noted. At these coordinates in the Dy405 images from the same field, relative intensity levels were measured using a constant sampling area for all cells within an experimental set. Using a 704 by 704 pixel image (314 by 314 μm) of each field, the size of the sample area in the *x*- and *y*-axes for each cell soma was adjusted according to the cell type morphology as follows: neurons, microglia/macrophages, T cells (12 × 12 pixels), natural killer cells (14 × 14 pixels), and astrocytes (8 × 8 pixels). For each cell type studied, all parameters were kept constant across the study.

Statistical Analysis

All statistical analyses were performed using Graphpad Prism 5. Analysis of global ATF3 protein levels for each animal was performed using Student's *t* test, and global *atf3* mRNA levels for each animal were determined using two-factor ANOVA and Bonferroni multiple comparisons post hoc analysis. As has been established in other in vivo studies investigating specific cellular responses (Bienvenu et al. 2012; Massi et al. 2012; Vianney-Rodrigues et al. 2011), cell-specific ATF3 protein signal intensity data from confocal microscopy were analyzed as per cell responses across multiple animals rather than condensing data from the individual cellular response to a global mean per animal. This is necessary as global means do not account for the variety of cellular responses across an injury field or the unequal number of cells per condition due to cellular loss or cellular proliferation. As the PBBI model is a severe penetrating brain injury encompassing 10 % of total brain volume and is computer-controlled, injury variability is minimized. In addition, inter-animal variability was controlled for by equal field location, size, and number for each animal.

Cell-specific data were analyzed using one-factor ANOVA and Dunn's multiple comparison post hoc analysis.

Results

Pooled mRNA from either sham controls or PBBI animals 24-h post-injury was analyzed using a targeted PCR array which included 83 transcription factors. Compared to sham levels, mRNAs for the transcription factor ATF3 were increased by sixfold (data not shown). In order to confirm that ATF3 levels were increased following PBBI injury, the protein levels were determined in sham controls and PBBI animals 24-h post-injury by Western blot. PBBI led to a 41 % increase ($p < 0.01$) in global ATF3 levels (Fig. 1).

The relative quantity of *atf3* mRNA for sham controls, PBBI animals, and PBBI animals treated with NNZ-2566 was measured at 4, 12, 24, 3, and 7 days post-injury (Fig. 2). PBBI alone caused a significant increase in *atf3* mRNA levels at all time points from 4 h through 3 days with a peak increase of over 13-fold at 12 h ($p < 0.001$). Except for the 4-h time point, all animals were treated for a period of 12 h with NNZ-2566. This treatment produced a further fourfold increase of *atf3* mRNA in comparison with PBBI alone ($p < 0.05$). Subsequently, *atf3* mRNA levels dropped precipitously, possibly due to the cessation of treatment, although levels were still significantly higher than sham controls ($p < 0.01$).

Since *atf3* mRNA levels were significantly increased at the 12-h time point (maximum time of drug treatment), protein expression levels were investigated at the 24-h time

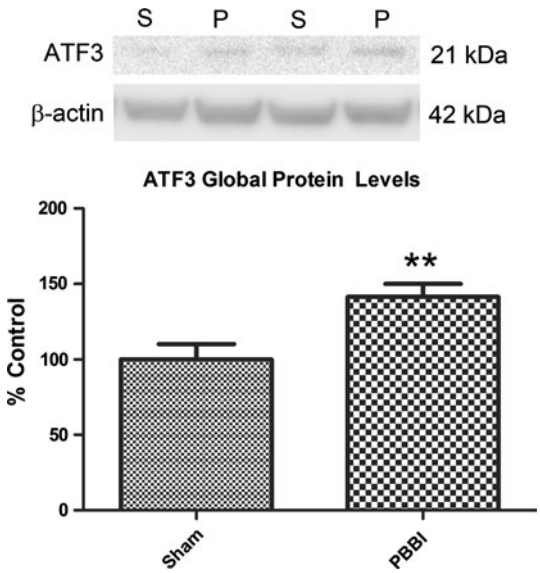

Fig. 1 ATF3 protein levels increase 24 h after PBBI. Protein levels from PBBI versus sham animals were quantified 24-h post-injury ($n = 8$). Representative bands for ATF3 and β-actin in sham (*S*) and PBBI (*P*) samples are shown at *top*. Quantification of band intensity presented as percent of control is shown *below*. Global ATF3 protein levels increased significantly in PBBI compared to sham controls (Student's *t* test, $^{**}p < 0.01$; *error bars* standard error of the mean)

point. ATF3 in microglia/macrophages was examined by co-staining with OX42. As expected, PBBI injury led to increased OX42 staining of activated microglia and infiltrating macrophages compared to sham animals (Fig. 3a, Supplemental Figure 2). Resting microglia in sham animals did not appear to express ATF3 (Fig. 3a, Supplemental Figure 2) and quantification of ATF3 expression in OX42-positive cells in sham animals confirmed that protein intensity levels were very low (Fig. 4). In contrast, activated microglia and macrophages (OX42-positive cells) at the injury site in PBBI animals clearly expressed ATF3 (Fig. 3a, Supplemental Figure 2). Quantification of microglia/macrophage-specific ATF3 protein intensity levels showed that PBBI alone led to an 820 % increase in ATF3 expression in these cells in comparison with sham controls (Fig. 4). NNZ-2566 treatment significantly increased ATF3 levels in these cell by an additional 102 % ($p < 0.001$) (Fig. 4).

ATF3 in T cells was examined using CD3. T cells in sham tissue were limited and appeared to be within vessels rather than in the CNS itself (Fig. 3b, Supplemental Figure 3). ATF3 expression in sham T cells was visible (Fig. 3b, Supplemental Figure 3). Quantification of ATF3 levels confirmed that T cells in shams had moderately high expression (Fig. 5). Unlike other cell types investigated, under PBBI conditions, ATF3 expression in T cells appeared to drop (Fig. 3b, Supplemental Figure 3). Quantification confirmed that ATF3 expression decreased by 48 % ($p < 0.001$) (Fig. 5). NNZ treatment reversed this, increasing levels by 107 % ($p < 0.001$) in comparison with PBBI levels and bringing levels back to those seen in normal tissue (i.e., comparable area in shams) (Fig. 5).

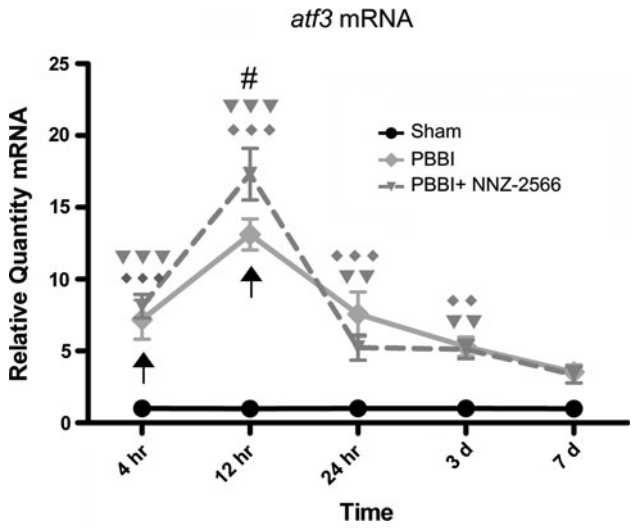

Fig. 2 NNZ-2566 treatment increases *atf3* mRNA levels in PBBI animals. The relative quantity of *atf3* mRNA at 4, 12, 24, 3, and 7 days ($n = 5$–6) for sham controls, PBBI animals, and animals treated with NNZ-2566 was evaluated using real-time PCR. *Arrows* indicate treatment termination time (two-factor ANOVA) $^{\blacklozenge}p < 0.05$; $^{\blacklozenge\blacklozenge}p < 0.01$; $^{\blacklozenge\blacklozenge\blacklozenge}p < 0.001$ (PBBI compared to Sham); $^{\blacktriangledown}p < 0.05$; $^{\blacktriangledown\blacktriangledown}p < 0.01$; $^{\blacktriangledown\blacktriangledown\blacktriangledown}p < 0.001$ (PBBI + NNZ-2566 compared to Sham); $^{\#}p < 0.05$ (PBBI + NNZ-2566 compared to PBBI). *Error bars* (standard error of the mean)

Immunostaining for NKC to study ATF3 expression in natural killer cells was completed. As expected, very few NKCs were visualized in normal brain tissue (shams) and those NKCs observed appeared to be within vessels rather than in the CNS. Under sham conditions, NKCs appeared to have only low expression of ATF3 (Fig. 3c, Supplemental Figure 4) and quantification confirmed that sham expression was modest (Fig. 6). Following PBBI, there was a clear infiltration of NKCs into the injury site (Fig. 3c, Supplemental Figure 4). Quantification of NKC ATF3 protein levels showed that PBBI alone led to a 58 % increase in ATF3 expression in these cells ($p < 0.01$). However, NNZ-2566 treatment significantly increased ATF3 levels in these cells by an additional 308 % ($p < 0.001$) (Fig. 6).

ATF3 protein localized to astrocytes was measured using GFAP. In normal sham tissue, ATF3 expression in astrocytes was rarely detectable by visual inspection through the microscope or of the image (20× objective) (Fig. 3D, Supplemental Figure 5). Quantification at the level of each astrocyte confirmed that expression was relatively low (Fig. 7) compared to the other cells studied. In PBBI animals, there was an increase in the number of activated astrocytes (astrogliosis) and also an increase in the number of astrocytes clearly expressing ATF3 (Fig. 3d, Supplemental Figure 5). Quantification of astrocyte-specific ATF3 expression levels showed that there was a 51 % increase in ATF3 levels in activated astrocytes from PBBI animals in comparison with non-activated sham astrocytes ($p < 0.001$). Treatment with NNZ-2566 further increased astrocytic expression of ATF3 by 13 % ($p < 0.001$) (Fig. 7).

Compared to the other cell types studied, neurons appeared to be the primary source of ATF3 expression in sham tissue (Fig. 3e, Supplemental Figure 6). Quantification confirmed that normal neuronal expression of ATF3 was greater than any of the other four cell types investigated under sham conditions (Fig. 8). Following PBBI, there was a decrease in the number of neurons at the injury site but those neurons that remained appeared to express more ATF3 (Fig. 3e, Supplemental Figure 6). Quantification of neuronal ATF3 expression intensity indicated that injury alone increased ATF3 expression levels by 55 % ($p < 0.001$) and that treatment with NNZ-2566 further increased ATF3 levels by 33 % ($p < 0.001$) (Fig. 8).

Discussion

Penetrating brain injury leads to immune cell activation and infiltration and pro-inflammatory cytokine release

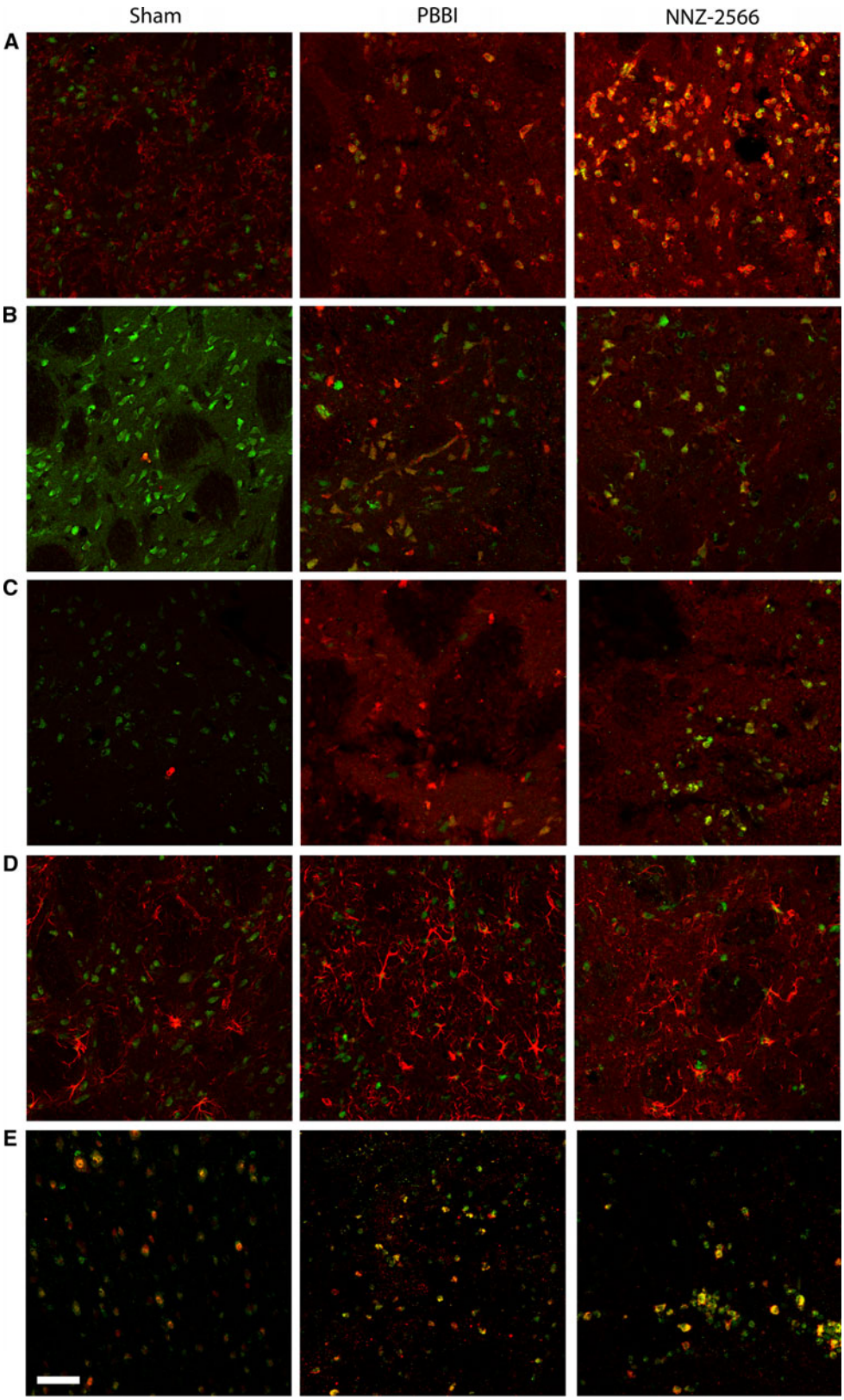

Fig. 3 Confocal microscopy of ATF3 protein expression in specific cell types in tissue from sham, PBBI, and NNZ-2566-treated PBBI animals 24-h post-injury. **a** Tissue was stained for ATF3 (*green*) and OX42 (*red*). **b** Tissue was stained with ATF3 (*green*) and CD3 (*red*). **c** Tissue was stained with ATF3 (*green*) and NKC (*red*). **d** Tissue was stained with ATF3 (*green*) and GFAP (*red*). **e** Tissue was stained with ATF3 (*green*) and NeuN (*red*) (*bar* = 50 μm)

(Wei et al. 2009; Williams et al. 2005, 2007). Previous studies in PBBI have demonstrated that post-injury treatment with NNZ-2566 can reverse increases in many pro-inflammatory cytokines, including TNF-α, IFN-γ, and IL6; however, the specific mechanism of action for this drug is not well defined (Wei et al. 2009). A review of the

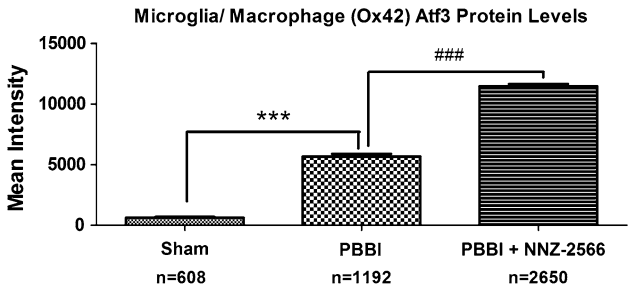

Fig. 4 NNZ-2566 increases ATF3 protein levels in microglia and macrophages 24-h post-injury. Levels of ATF3 in microglia and macrophages from the injury site of PBBI and NNZ-2566-treated PBBI animals were compared to levels in those found in sham animals (one-factor ANOVA, $^{***}p < 0.001$ compared to sham, $^{\#\#\#}p < 0.001$ compared to PBBI). *Error bars* (standard error of the mean)

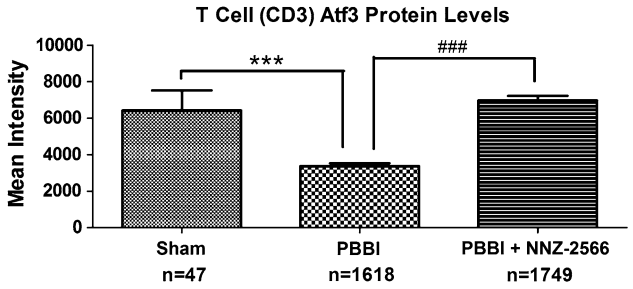

Fig. 5 NNZ-2566 increases Aft3 protein levels in T cells 24-h post-injury. Levels of Atf3 in T cells from the injury site of PBBI and NNZ-2566-treated PBBI animals were compared to levels in those found in sham animals (one-factor ANOVA, $^{***}p < 0.001$ compared to sham, $^{\#\#\#}p < 0.001$ compared to PBBI). *Error bars* (standard error of the mean)

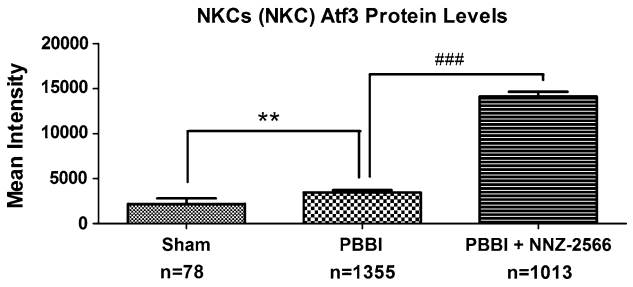

Fig. 6 NNZ-2566 increases ATF3 protein levels in natural killer cells 24-h post-injury. Levels of ATF3 in NKCs from the injury site of PBBI and NNZ-2566-treated PBBI animals were compared to levels in those found in sham animals (one-factor ANOVA, $^{**}p < 0.01$ compared to sham, $^{\#\#\#}p < 0.001$ compared to PBBI). *Error bars* (standard error of the mean)

literature suggests that pro-inflammatory cytokines are under the regulation of ATF3 which functions as a transcription repressor (Litvak et al. 2009; Rosenberger et al. 2008). Increased *atf3* mRNA levels have been seen in multiple models of TBI (Israelsson et al. 2008; Natale et al. 2003) suggesting that it may function as an internal survival mechanism as the brain itself seeks to control

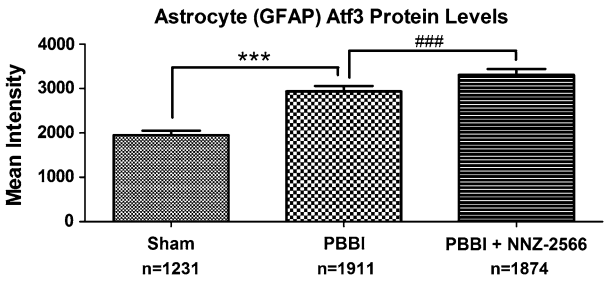

Fig. 7 NNZ-2566 increases ATF3 protein levels in astrocytes 24-h post-injury. Levels of ATF3 in astrocytes from the injury site of PBBI and NNZ-2566-treated PBBI animals were compared to levels in those found in sham animals (one-factor ANOVA, $^{***}p < 0.001$ compared to sham, $^{\#\#\#}p < 0.001$ compared to PBBI). *Error bars* (standard error of the mean)

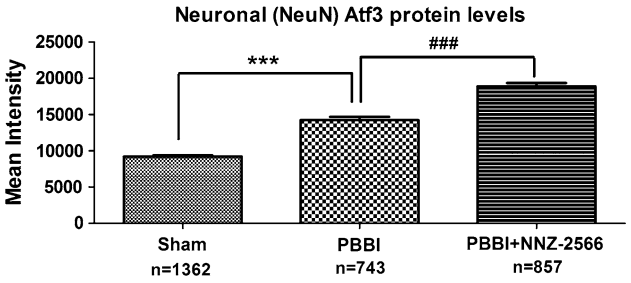

Fig. 8 NNZ-2566 increases ATF3 protein levels in neurons 24-h post-injury. Levels of ATF3 in neurons from the injury site of PBBI and NNZ-2566-treated PBBI animals were compared to levels in those found in sham animals (one-factor ANOVA, $^{***}p < 0.001$ compared to sham, $^{\#\#\#}p < 0.001$ compared to PBBI). *Error bars* (standard error of the mean)

ongoing injury-induced inflammation. In this study, we report that by array analysis, mRNA levels of the transcription factor ATF3 increase over sixfold at 24-h post-PBBI and by more detailed temporal quantitative PCR analysis that PBBI injury alone significantly upregulates *atf3* mRNA levels within 4-h post-injury and that mRNA levels remain elevated through 3 days post-injury, peaking at 12 h. In addition, at 24-h post-PBBI, there is a 41 % increase in global ATF3 protein levels. Together, these findings indicate that ATF3 plays an important role in regulating post-PBBI events and may assist in the suppression of early onset pro-inflammatory cytokines such as TNF-α or IL-6 (Wei et al. 2009).

Our goal was to examine a possible specific step in the mechanism of neuroprotective action of the drug NNZ-2566 in a model of PBBI and to determine whether this treatment alters the endogenous post-PBBI changes in ATF3 expression. NNZ-2566 treatment was initiated 30-min post-injury and continued through 12-h post-injury. This treatment significantly increased *atf3* mRNA levels beyond that seen with PBBI alone. Hence, these NNZ-2566-induced changes in *atf3* measures may indeed be responsible for the decreases in pro-inflammatory cytokine

levels previously demonstrated with NNZ-2566 treatment for PBBI rats (Wei et al. 2009).

Precipitously decreased mRNA levels were measured beyond 12-h post-injury with the cessation of NNZ-2566 treatment, although these levels were still similar to those of injury alone. Clinical studies investigating treatments aimed at reducing secondary damage following TBI continue treatment for several days, (ANZICRC_Clinical_Study 2009; BHRP_Clinical_Study 2010) allowing for continued treatment for a greater portion of the acute inflammation stage. In fact, in the ongoing Phase II clinical trial, NNZ-2566 is being administered continuously for 3 days post-injury (Neuren_Clinical_Study 2008). However, in this study, we restricted the treatment time to allow for direct comparisons to our previous measures of NNZ-2566 effects on cytokine levels (Wei et al. 2009). The identification of a drop in mRNA levels following cessation of the drug offers further validation that continued NNZ-2566 treatment beyond 12 h may allow for longer-term increases in *atf3* mRNA and in turn significant therapeutic benefit (Lu et al. 2009a).

The changes described in Figs. 1 and 2 measure global changes in ATF3 protein or *atf3* mRNA levels and therefore do not allow us to determine what cell types contribute to the increases seen. We therefore quantified cell-type-specific ATF3 protein levels after NNZ-2566 treatment for PBBI, looking first at the immune cells known to express pro-inflammatory cytokines and that have previously been shown to be regulated by ATF3 (Thompson et al. 2009). Because the blood–brain barrier is highly compromised in the PBBI model due to the penetration of the brain, both infiltrating macrophages and activation of resident microglia are expected in this injury and these cells share similar marker expression. Similar to what has been previously shown (Williams et al. 2007), microglial/macrophage activation was indeed widespread at the injury site at 24-h post-injury (Fig. 3a, Supplemental Figure 2). Activated microglia and infiltrating macrophages have phagocytic function necessary for the clearing of cellular debris at the injury site (Tambuyzer et al. 2009). In addition, they secrete pro-inflammatory cytokines, such as IL-1, TNF-α, IFN-γ, and IL-6, involved in autocrine activation of microglia and macrophages and in paracrine attraction and activation of leukocytes (Stow et al. 2009; Tambuyzer et al. 2009). Importantly, activated microglia have also been shown to produce anti-inflammatory cytokines IL-10, TGF-β, and IL-1ra, showing they may also be involved in limiting inflammatory mechanisms (Tambuyzer et al. 2009). Here, we found that injury alone increased ATF3 levels by 820 % in microglia and macrophages and that NNZ-2566 was able to significantly increase ATF3 protein levels by an additional 102 %. We did not see a reduction in the number of cells per field, suggesting that NNZ-2566 induction of ATF3 may reduce inflammatory cytokine production in these cells but allow for other important functions such as phagocytosis.

Studies of severe TBI in humans indicate that the T cells that infiltrate the injury area are mainly $CD8^+$ T cells and that absolute $CD4^+$ T cells levels are suppressed (Mazzeo et al. 2006). Few T cells are found in normal animals, and these are seemingly limited to vessels rather than CNS tissue. This is to be expected since T cell infiltration of normal brain is known to be highly limited. However, within 24 h of the penetrating brain injury, T cell infiltration was present, and although in our study the subclass of T cell was not determined, based on the human data, it is likely that these are primarily $CD8^+$ T cells which are recognized for their ability to induce cytolysis in infected cells (Harty et al. 2000). Cytotoxic T cell infiltration of the brain is most often studied in situations of autoimmune CNS disease or infection (Schroeter and Jander 2005) but their function in severe TBI is not well understood. However, it is known that in addition to cytolysis, $CD8^+$ T cells produce IFN-γ and TNF and that these can facilitate local macrophage activation (Harty et al. 2000). In PBBI, we found that ATF3 expression was significantly decreased by 48 % in comparison with that seen in sham tissue. Treatment with NNZ-2566 was able in increased ATF3 levels by 107 % over that seen with PBBI alone, and thus return T cell expression of ATF3 to levels comparable to that seen in sham tissue. The reduction of ATF3 levels in T cells with injury alone suggests that T cells may be an important source of increased pro-inflammatory cytokine release in penetrating injury. Conversely, increased ATF3 expression with NNZ-2566 treatment may assist in controlling T cell-derived pro-inflammatory cytokine levels following injury.

Few studies have looked at the role of NKCs in TBI. Similar to T cells, NKCs are not usually found in normal brain. However, it is known that, especially in cases of CNS injury where the blood–brain barrier is compromised, activated NKCs infiltrate the injury area (Byram et al. 2003; Hammarberg et al. 2000; Matsumoto et al. 1998; Raivich et al. 1998). Following PBBI, there was significant NKC infiltration 24-h post-injury and ATF3 levels within these NKCs were increased significantly. However, the increase with injury alone was relatively small compared to the dramatic increase (308 %) seen in injured animals treated with NNZ-2566. NKCs express several of the pro-inflammatory cytokines that are markers of TBI, including TNF-α, IFN-γ, and IL-6 (Fauriat et al. 2010; Perussia 1996). Therefore, the increase in ATF3 expression with NNZ-2566 treatment could be expected to decrease NKC derived pro-inflammatory cytokine levels.

Astrocytes serve critical roles in glutamate homeostasis, and normal astrocyte function is necessary for normal neuronal signaling and to prevent excitotoxicity caused by

excessive glutamate release into neuronal synapses (Schousboe and Waagepetersen 2005; Chen and Swanson 2003). As shown here, following PBBI (Fig. 3d, Supplemental Figure 5) and elsewhere (Cartagena et al. 2008; Stoica et al. 2009), astrocyte activation (astrogliosis) is a signature feature of TBI. However, whether astrogliosis is beneficial or detrimental remains a point of debate. Astrocytes are capable of expressing MHC class II and co-stimulatory molecules B7 and CD40, showing that they are antigen-presenting cells (APCs) and indicating a direct role of astrocytes in the T cell immune response (Dong and Benveniste 2001). Following either ischemic or traumatic injury, astrocytes have been shown to release pro-inflammatory cytokines IL1α, TNF-α, IFN-γ, and IL-6 (Lau and Yu 2001). However, the experimental inhibition of astrogliosis following TBI resulted in increased lesion volume, (Myer et al. 2006) showing astrogliosis also has potential and critical beneficial functions. PBBI induced significant increases in ATF3 expression in astrocytes following injury. Although the astrocyte levels of ATF3 under all conditions were low in comparison with other cell types, NNZ-2566 treatment still caused a significant 13 % increase in expression in comparison with PBBI alone, suggesting that NNZ-2566 has a global effect on multiple cell types resulting in increased ATF3 expression. Treatment with NNZ-2566 for 12 h did not eliminate astrogliosis in this model; however, the reduction in pro-inflammatory cytokine release by NNZ-2566 could allow for other beneficial astrocytic functions while controlling detrimental inflammation.

The neuroprotective properties of NNZ-2566 may be related primarily to the suppression of pro-inflammatory cytokine production (Wei et al. 2009). We have previously shown that NNZ-2566 treatment for PBBI under the same conditions as this study leads to decreased levels of IL-6, TNF-α, and IFN-γ, as well as other pro-inflammatory cytokines (Wei et al. 2009). The findings here suggest that one mechanism leading to decreased pro-inflammatory cytokine release involves increased ATF3 signaling in these cytokine-producing cells types. However, it is also likely that NNZ-2566 is affecting ATF3 levels in neurons themselves. Indeed, increased ATF3 levels have been shown in neurons following axonal injury (Seijffers et al. 2006) and after excitotoxic stimuli (Francis et al. 2004; Zhang et al. 2011). Furthermore, in vitro overexpression of ATF3 has been shown to protect neurons from apoptosis induced by growth factor withdrawal or staurosporine exposure (Zhang et al. 2011), or kainic acid exposure (Francis et al. 2004). In vivo overexpression of ATF3 through adeno-associated virus delivery to the brain was able to protect neurons following cerebral ischemic insult (Zhang et al. 2011). Here, we established that in normal tissue, neuronal levels of ATF3 were very high in comparison with other cell types, suggesting that ATF3 may serve an important function in maintaining neuronal integrity. Since following PBBI, there was a measured overexpression of ATF3 one might speculate that an innate neuronal survival mechanism exists related to some as yet, undetermined, ATF3-regulated genes. NNZ-2566 treatment led to an additional 33 % increase in neuronal ATF3 expression suggesting that NNZ-2566 can directly enhance this protective neuronal mechanism.

Activating transcription factor-3 is known to reduce inflammation (Litvak et al. 2009; Rosenberger et al. 2008; Thompson et al. 2009) and protect neurons from apoptosis and excitotoxicity (Francis et al. 2004; Zhang et al. 2011). Following PBBI, ATF3 was significantly increased in microglia, macrophages, NKCs, astrocytes, and neurons, indicating that this protective mechanism can be activated by injury alone and may represent an attempt by the CNS itself to control injury-induced inflammation and neuronal death. Interestingly, injury alone was not able to increase ATF3 levels in T cells. In fact, levels decreased precipitously, potentially leading to uncontrolled pro-inflammatory cytokine release from these cells. Here, NNZ-2566 treatment for 12 h succeeded in increasing ATF3 expression in multiple inflammatory and glial cell types, including T cells, while at the same time also increasing its expression in neurons. This establishes that NNZ-2566 has effects on ATF3 expression in multiple cell types and its neuroprotective effects may therefore be due to a combined effect of reduced pro-inflammatory release from immune cells and glia, (Lu et al. 2009a; Wei et al. 2009) as well as the direct protection of neurons through increased neuronal ATF3 expression.

Although NNZ-2566 treatment was able to preserve neuronal circuitry as indicated by improved behavioral outcome measures and reduced non-convulsive seizure incidence, it did not reduce lesion volume in the PBBI model (Lu et al. 2009a). However, this is a severe penetrating model affecting 10 % of total brain volume. In the MCAO model, NNZ-2566 treatment resulted in a significant reduction in infarct volume showing that NNZ-2566-induced mechanisms can preserve neuronal tissue (Lu et al. 2009b). For both models, ATF3 induction in neurons following NNZ-2566 treatment would explain the improvements seen in the preservation of neuronal circuitry; beneficial effects measured with a relatively short treatment window of 12 h. Given that inflammatory mechanisms continue well beyond this time point, it is likely that prolonged NNZ-2566 treatment would have additional protective effects. Consistent with this hypothesis, ATF3 transcription is known to be upregulated following in vitro stimulation of a variety of TLRs at the surface (Gilchrist et al. 2006; Litvak et al. 2009; Whitmore et al. 2007). Future studies may determine whether the effect of

NNZ-2566 on ATF3 expression is direct or through interaction with surface receptors such as TLRs.

Acknowledgments We would like to thank Matthew Bombard and Weihong Yang for their excellent assistance with surgical procedures. These studies were supported in part by a cooperative research and development agreement with Neuren Pharmaceuticals Ltd. (W81XWH-05-0074). This material has been reviewed by the Walter Reed Army Institute of Research. There is no objection to its presentation and/or publication. The opinions or assertions contained herein are the private views of the authors and are not to be construed as official, or reflecting true views of the Department of the Army or the Department of Defense.

Conflict of interest No competing financial interests exist.

References

Amiry-Moghaddam, M., Otsuka, T., Hurn, P. D., Traystman, R. J., Haug, F. M., Froehner, S. C., et al. (2003). An alpha-syntrophin-dependent pool of AQP4 in astroglial end-feet confers bidirectional water flow between blood and brain. *Proceedings of the National Academy of Sciences of the United States of America, 100*(4), 2106–2111.

Bickerdike, M. J., Thomas, G. B., Batchelor, D. C., Sirimanne, E. S., Leong, W., Lin, H., et al. (2009). NNZ-2566: A Gly-Pro-Glu analogue with neuroprotective efficacy in a rat model of acute focal stroke. *Journal of the Neurological Sciences, 278*(1–2), 85–90.

Bienvenu, T. C., Busti, D., Magill, P. J., Ferraguti, F., & Capogna, M. (2012). Cell-type-specific recruitment of amygdala interneurons to hippocampal theta rhythm and noxious stimuli in vivo. [Research Support, Non-U.S. Gov't]. *Neuron, 74*(6), 1059–1074.

Byram, S. C., Serpe, C. J., Pruett, S. B., Sanders, V. M., & Jones, K. J. (2003). Natural killer cells do not mediate facial motoneuron survival after facial nerve transection. *Brain, Behavior, and Immunity, 17*(6), 417–425.

Cartagena, C. M., Ahmed, F., Burns, M. P., Pajoohesh-Ganji, A., Pak, D. T., Faden, A. I., et al. (2008). Cortical injury increases cholesterol 24S hydroxylase (Cyp46) levels in the rat brain. *Journal of Neurotrauma, 25*(9), 1087–1098.

Chen, B. P., Liang, G., Whelan, J., & Hai, T. (1994). ATF3 and ATF3 delta Zip. Transcriptional repression versus activation by alternatively spliced isoforms. *Journal of Biological Chemistry, 269*(22), 15819–15826.

Chen, Y., & Swanson, R. A. (2003). Astrocytes and brain injury. *Journal of Cerebral Blood Flow and Metabolism, 23*(2), 137–149.

Dong, Y., & Benveniste, E. N. (2001). Immune function of astrocytes. *Glia, 36*(2), 180–190.

Efficacy and Safety Study of Intravenous Progesterone in Patients with Severe Traumatic Brain Injury (SyNAPSe). (2010). *BHR Pharma, LLC*. Accessed July 9, 2012 from http://www.clinicaltrials.gov/ct2/show/NCT01143064?term=nct01143064&rank=1.

Erythropoietin in Traumatic Brain Injury (EPO-TBI). (2009). *Australian and New Zealand Intensive Care Research Centre*. Accessed July 9, 2012 from http://www.clinicaltrials.gov/ct2/show/NCT00987454?term=nct00987454&rank=1.

Fauriat, C., Long, E. O., Ljunggren, H. G., & Bryceson, Y. T. (2010). Regulation of human NK-cell cytokine and chemokine production by target cell recognition. *Blood, 115*(11), 2167–2176.

Francis, J. S., Dragunow, M., & During, M. J. (2004). Over expression of ATF-3 protects rat hippocampal neurons from in vivo injection of kainic acid. *Brain Research. Molecular Brain Research, 124*(2), 199–203.

Gilchrist, M., Thorsson, V., Li, B., Rust, A. G., Korb, M., Roach, J. C., et al. (2006). Systems biology approaches identify ATF3 as a negative regulator of Toll-like receptor 4. *Nature, 441*(7090), 173–178.

Hammarberg, H., Lidman, O., Lundberg, C., Eltayeb, S. Y., Gielen, A. W., Muhallab, S., et al. (2000). Neuroprotection by encephalomyelitis: Rescue of mechanically injured neurons and neurotrophin production by CNS-infiltrating T and natural killer cells. *Journal of Neuroscience, 20*(14), 5283–5291.

Harty, J. T., Tvinnereim, A. R., & White, D. W. (2000). $CD8^+$ T cell effector mechanisms in resistance to infection. *Annual Review of Immunology, 18*, 275–308.

Israelsson, C., Bengtsson, H., Kylberg, A., Kullander, K., Lewen, A., Hillered, L., et al. (2008). Distinct cellular patterns of upregulated chemokine expression supporting a prominent inflammatory role in traumatic brain injury. *Journal of Neurotrauma, 25*(8), 959–974.

Lau, L. T., & Yu, A. C. (2001). Astrocytes produce and release interleukin-1, interleukin-6, tumor necrosis factor alpha and interferon-gamma following traumatic and metabolic injury. *Journal of Neurotrauma, 18*(3), 351–359.

Litvak, V., Ramsey, S. A., Rust, A. G., Zak, D. E., Kennedy, K. A., Lampano, A. E., et al. (2009). Function of C/EBPdelta in a regulatory circuit that discriminates between transient and persistent TLR4-induced signals. *Nature Immunology, 10*(4), 437–443.

Lu, X. C., Chen, R. W., Yao, C., Wei, H., Yang, X., Liao, Z., et al. (2009a). NNZ-2566, a glypromate analog, improves functional recovery and attenuates apoptosis and inflammation in a rat model of penetrating ballistic-type brain injury. *Journal of Neurotrauma, 26*(1), 141–154.

Lu, X. C., Hartings, J. A., Si, Y., Balbir, A., Cao, Y., & Tortella, F. C. (2011). Electrocortical pathology in a rat model of penetrating ballistic-like brain injury. *Journal of Neurotrauma, 28*(1), 71–83.

Lu, X. C., Si, Y., Williams, A. J., Hartings, J. A., Gryder, D., & Tortella, F. C. (2009b). NNZ-2566, a glypromate analog, attenuates brain ischemia-induced non-convulsive seizures in rats. *Journal of Cerebral Blood Flow and Metabolism, 29*(12), 1924–1932.

Massi, L., Lagler, M., Hartwich, K., Borhegyi, Z., Somogyi, P., & Klausberger, T. (2012). Temporal dynamics of parvalbumin-expressing axo-axonic and basket cells in the rat medial prefrontal cortex in vivo. [Research Support, Non-U.S. Gov't]. *Journal of Neuroscience, 32*(46), 16496–16502.

Matsumoto, Y., Kohyama, K., Aikawa, Y., Shin, T., Kawazoe, Y., Suzuki, Y., et al. (1998). Role of natural killer cells and TCR gamma delta T cells in acute autoimmune encephalomyelitis. *European Journal of Immunology, 28*(5), 1681–1688.

Mazzeo, A. T., Kunene, N. K., Gilman, C. B., Hamm, R. J., Hafez, N., & Bullock, M. R. (2006). Severe human traumatic brain injury, but not cyclosporin a treatment, depresses activated T lymphocytes early after injury. *Journal of Neurotrauma, 23*(6), 962–975.

Myer, D. J., Gurkoff, G. G., Lee, S. M., Hovda, D. A., & Sofroniew, M. V. (2006). Essential protective roles of reactive astrocytes in traumatic brain injury. *Brain, 129*(Pt 10), 2761–2772.

Natale, J. E., Ahmed, F., Cernak, I., Stoica, B., & Faden, A. I. (2003). Gene expression profile changes are commonly modulated across models and species after traumatic brain injury. *Journal of Neurotrauma, 20*(10), 907–927.

Perussia, B. (1996). The cytokine profile of resting and activated NK cells. *Methods, 9*(2), 370–378.

Raivich, G., Jones, L. L., Kloss, C. U., Werner, A., Neumann, H., & Kreutzberg, G. W. (1998). Immune surveillance in the injured nervous system: T-lymphocytes invade the axotomized mouse facial motor nucleus and aggregate around sites of neuronal degeneration. *Journal of Neuroscience, 18*(15), 5804–5816.

Rosenberger, C. M., Clark, A. E., Treuting, P. M., Johnson, C. D., & Aderem, A. (2008). ATF3 regulates MCMV infection in mice by modulating IFN-gamma expression in natural killer cells. *Proceedings of the National Academy of Sciences of the United States of America, 105*(7), 2544–2549.

Saura, J., Curatolo, L., Williams, C. E., Gatti, S., Benatti, L., Peeters, C., et al. (1999). Neuroprotective effects of Gly-Pro-Glu, the N-terminal tripeptide of IGF-1, in the hippocampus in vitro. *Neuroreport, 10*(1), 161–164.

Schousboe, A., & Waagepetersen, H. S. (2005). Role of astrocytes in glutamate homeostasis: Implications for excitotoxicity. *Neurotoxicity Research, 8*(3–4), 221–225.

Schroeter, M., & Jander, S. (2005). T-cell cytokines in injury-induced neural damage and repair. *Neuromolecular Medicine, 7*(3), 183–195.

Seijffers, R., Allchorne, A. J., & Woolf, C. J. (2006). The transcription factor ATF-3 promotes neurite outgrowth. *Molecular and Cellular Neuroscience, 32*(1–2), 143–154.

Stoica, B., Byrnes, K., & Faden, A. I. (2009). Multifunctional drug treatment in neurotrauma. *Neurotherapeutics, 6*(1), 14–27.

Stow, J. L., Low, P. C., Offenhauser, C., & Sangermani, D. (2009). Cytokine secretion in macrophages and other cells: Pathways and mediators. *Immunobiology, 214*(7), 601–612.

Study of NNZ-2566 in Patients with Traumatic Brain Injury (INTREPID2566). (2008). *Neuren Pharmaceuticals*. Accessed July 9, 2012 from http://www.clinicaltrials.gov/ct2/show/NCT00805818?term=NNZ&rank=4.

Tambuyzer, B. R., Ponsaerts, P., & Nouwen, E. J. (2009). Microglia: Gatekeepers of central nervous system immunology. *Journal of Leukocyte Biology, 85*(3), 352–370.

Thompson, M. R., Xu, D., & Williams, B. R. (2009). ATF3 transcription factor and its emerging roles in immunity and cancer. *Journal of Molecular Medicine (Berlin, Germany), 87*(11), 1053–1060.

Vianney-Rodrigues, P., Iancu, O. D., & Welsh, J. P. (2011). Gamma oscillations in the auditory cortex of awake rats. [Research Support, N.I.H., Extramural Research Support, Non-U.S. Gov't]. *European Journal of Neuroscience, 33*(1), 119–129.

Wei, H. H., Lu, X. C., Shear, D. A., Waghray, A., Yao, C., Tortella, F. C., et al. (2009). NNZ-2566 treatment inhibits neuroinflammation and pro-inflammatory cytokine expression induced by experimental penetrating ballistic-like brain injury in rats. *Journal of Neuroinflammation, 6*, 19.

Whitmore, M. M., Iparraguirre, A., Kubelka, L., Weninger, W., Hai, T., & Williams, B. R. (2007). Negative regulation of TLR-signaling pathways by activating transcription factor-3. *Journal of Immunology, 179*(6), 3622–3630.

Williams, A. J., Hartings, J. A., Lu, X. C., Rolli, M. L., Dave, J. R., & Tortella, F. C. (2005). Characterization of a new rat model of penetrating ballistic brain injury. *Journal of Neurotrauma, 22*(2), 313–331.

Williams, A. J., Hartings, J. A., Lu, X. C., Rolli, M. L., & Tortella, F. C. (2006a). Penetrating ballistic-like brain injury in the rat: Differential time courses of hemorrhage, cell death, inflammation, and remote degeneration. *Journal of Neurotrauma, 23*(12), 1828–1846.

Williams, A. J., Ling, G. S., & Tortella, F. C. (2006b). Severity level and injury track determine outcome following a penetrating ballistic-like brain injury in the rat. *Neuroscience Letters, 408*(3), 183–188.

Williams, A. J., Wei, H. H., Dave, J. R., & Tortella, F. C. (2007). Acute and delayed neuroinflammatory response following experimental penetrating ballistic brain injury in the rat. *Journal of Neuroinflammation, 4*, 17.

Zhang, S. J., Buchthal, B., Lau, D., Hayer, S., Dick, O., Schwaninger, M., et al. (2011). A signaling cascade of nuclear calcium-CREB-ATF3 activated by synaptic NMDA receptors defines a gene repression module that protects against extrasynaptic NMDA receptor-induced neuronal cell death and ischemic brain damage. *Journal of Neuroscience, 31*(13), 4978–4990.